Technical Paper

ISSN 1997-1400 Int. J. Pavement Res. Technol. 7(1):49-59
Copyright @ Chinese Society of Pavement Engineering

Non Dowel Joint Spacing for Low Volume Roads in Tropical Climate - A case study in Sri Lanka

A.M.A.N. Karunarathne[1], W.K. Mampearachchi[2+], and S.M.A. Nanayakkara[2]

Abstract: Shrinkage and thermal stresses are the dominant contributors to develop tensile stresses in rigid pavements. As a result, cracks can be developed in pavement without vehicle loading. Providing lateral joints at appropriate spacing is one of the solutions to overcome the said stresses. Width of a joint will be wider at the time when curling and contraction strains are at the optimum strain. It is essential to consider daily temperature variation, shrinkage and curling together with the fatigue damage in determination of optimum joint spacing for concrete roads.

Rigid pavements are usually exposed to solar radiation to a great extent and as a result thermal stresses are developed. This research propose a methodology to estimate the relevant deformation (width of the joint) of concrete due to its exposure to the solar radiation incorporate the temperature variation of the concrete slab by use of a 3D finite element model (FEM) approach. A laboratory scale slab was used to verify the results obtained from the FEM. Lateral deformations due to shrinkage effect were calculated according to the American Concrete Institute shrinkage model (ACI 209 R-92).

Aggregate interlocking is an efficient load transfer mechanism for thin concrete pavements which are commonly used in rural roads. An Experiment was carried out to find a relationship between crack width of the interlocking joint and load transfer efficiency (LTE). From the obtained results, it was observed that LTE decreases non-linearly with the increase of crack width. According to the study, joint spacing of thin rigid pavements can be provided even beyond the specified values of American Concrete Pavement Association (ACPA) to maintain 60% of LTE.

DOI:10.6135/ijprt.org.tw/2014.7(1).49

***Key words**: FEM; Joint spacing; LT; Rigid pavement; Shrinkage.*

Introduction

Five to six inches thick rigid pavements with grade 25 -30 concrete are sufficient to serve the low volume roads having annual truck/ bus traffic less than 50000 [1]. Concrete has lower tensile and flexural strengths; therefore concrete cannot be deformed as flexible road paving materials [2]. Hence, concrete roads have to be designed in such a way that the induced flexural stresses would not exceed the threshold limits for designed traffic. Developed flexural stresses can be confined by providing lateral joints at appropriate intervals. This will disconnect the pavement slab. When the connectivity fails at a joint location, load of wheel at the joint has to be carried by one of the slabs. This leads to distresses and joint failures in the pavements. Therefore, adequate load transfer should be maintained at the joints. Aggregate interlocking in transverse joints is the ideal mechanism of load transferring in thin concrete slabs for rural roads compared to the dowel bar insertion [3].

Concrete will crack due to drying shrinkage and thermal movements and it is possible to induce cracks at predetermined locations by making the concrete section weaker at those locations. Shrinkage is the main disadvantage of concrete pavement over the flexible pavements. Shrinkage cannot be completely prevented in any concrete construction. It will govern the performance of rigid pavements as they are exposed to severe environmental effects throughout its life span. As a result, shrinkage cracks can occur transversely through the slab width. Although these transverse cracks cannot be eliminated, it is possible to obtain the required load transfer at those cracks. In order to achieve this, the width of the propagated crack should be limited to accommodate proper aggregate interlock. Interlocking of aggregates stands at a cracked concrete section when the two parts are close enough to each other.

Effectiveness of aggregate interlocking mechanism depends on the strength of the concrete, strength of aggregate, maximum aggregate size, the wheel load, slab thickness and joint opening [4]. Crack width depends on ultimate shrinkage strain and curling of concrete slabs due to daily temperature variation. Daily variation of concrete temperature governs the expansion and curling of concrete slabs. In tropical countries, there are seasonal differences in monthly rainfall, whereas the temperature variation is fairly constant throughout the year [5]. Therefore, daily temperature variation is the critical factor for thermal deformations of concrete than seasonal variation of the climate. Therefore, the concrete pavements are subjected to continuous curling and warping causing fatigue. It reduces the connectivity at joints of adjacent slab panels as concrete expands under higher temperatures and contracts under lower temperatures. Width of a transverse crack will be wider at the time when curling and contraction strains are at the optimum strain. It is essential to consider daily temperature variation, shrinkage and curling together with the fatigue damage in determination of optimum joint spacing for low volume roads.

Pavement design procedures such as AASHTO Procedure for Low Volume Roads [6] and the Portland Cement Association

[1] Swinburne University of Technology, Australia.
[2] University of Moratuwa, Sri Lanka.
[+] Corresponding Author: E-mail wasanthak@civil.mrt.ac.lk
Note: Submitted December 28, 2012; Revised May 23, 2013; Accepted July 2, 2013.

procedure [7] show very little difference in thickness requirements between undoweled and doweled pavements for thicknesses of 7 in. (175 mm) or less. In the few cases where there is a slight difference, the use of dowels would not be a cost-effective trade-off for a small increase in slab thickness. This concept is accepted by several agencies [8-10] and recommends plain, undoweled pavements of slab thicknesses less than 200 mm (8 in) for light traffic roads.

Rigid pavements are exposed to severe environment effects during the entire life. Results of previous analysis [11, 12] have indicated that when the temperature differential in the slab is positive, causing the slab to curl upward at the center which creates the critical loading position is at the center of the slab. When the temperature differential is negative, the critical loading position is at the corner of the slab. When these two thermal conditions were used for computation of critical stresses, it was found that, for the same applied load, the positive thermal gradient condition produced substantially higher stresses [6]. Study conducted by Tia et al [13] concluded that the computed maximum stress is unaffected by the change of slab length with a temperature differential less than +5°F (2.7°C). Temperature differential in 150 mm thick concrete slab has been recorded above +5°F (2.7°C) from 10 AM to 4.00 PM during a typical day in Sri Lanka [14]. Therefore, the joint spacing selection needs to be rest on temperature gradients in slab as well as the shrinkage of concrete.

In plain jointed concrete pavements, the joint is designed to create a weakness plane that will control the formation of transverse cracks. The weak plane will allow forming a shrinkage induced crack which provided at desired location. Table 1 shows the joint spacing for various pavement thicknesses recommended by ACPA [7]. Typically, for jointed plain concrete streets, the joint spacing should be 24 to 30 times the pavement thickness with the maximum spacing of 15 ft (4.5 m). It is also important to keep slabs as square as possible and the transverse joint spacing should not exceed 125% to 150% of the longitudinal joint spacing [7]. Table 1 shows that 3.7 m - 4.6 m joint spacing is recommended as appropriate for rigid pavements with 150 mm thickness.

Undesirable cracks in the rigid pavements influence its performance. Primary purpose of transverse contraction joints is to control the unwanted cracking that results from the tensile and bending stresses in concrete slabs caused by the drying shrinkage, traffic loadings, and ambient temperature variation. A distressed joint typically exhibits faulting and/or spalling. Poor joint performance frequently leads to further distresses such as corner breaks, blowups, and mid-panel cracks. Such cracks may themselves begin to function as joints and develop similar distresses.

Descriptive procedures are not provided in available guidelines [6, 7] to select the suitable joint spacing for undoweled joints where load transfer is relying on the aggregate interlocking. This study considers the shrinkage of concrete and load transfer efficiency in undoweled plane concrete pavements and provides a procedure to design the joint spacing. Fig. 1 shows the flow chart of the study described in this paper.

Table 1. Joint Spacing for Plain Concrete Pavements Recommended by ACPA [7].

Pavement Thickness, mm (in)	Joint Spacing, m (ft)
125 (5 in)	3.0 -3.8 (10 -12.5 ft)
150 (6 in)	3.7 – 4.6 (12 – 15 ft)
175 (7 in)	4.3 – 4.6 (14 – 15 ft)
200 (8 in)	4.6 (15 ft)

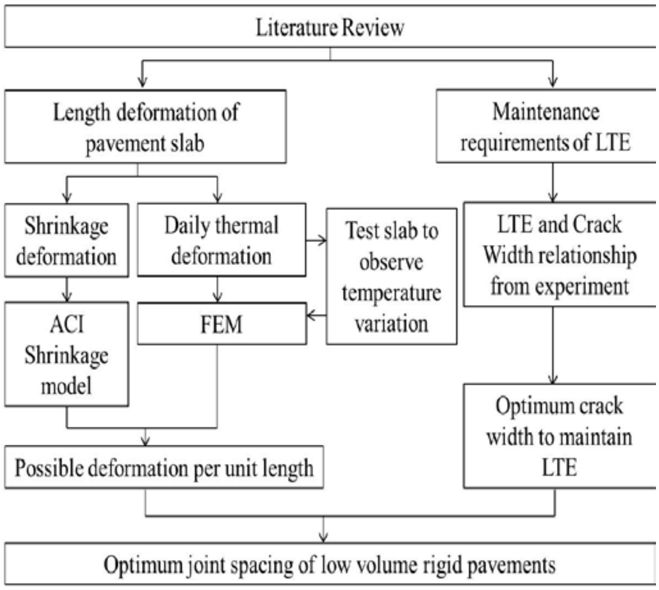

Fig. 1. Flow Chart of the Study.

Deformation Due to Daily Thermal Variation

Solar Radiation Variation in Tropics

Standard solar radiation meter measures the total solar radiation falls on the 1 m2 area on the earth surface. Al-Dallal and Zein [15] have measured the solar radiation drop on ground surface in Bahrain and were able to divide the total radiation values into its major components as visible rays and infrared rays. These results are in the form of sinusoidal variation with a peak of 950 W/m^2.

In this study, a sinusoidal variation with a peak value of 900 W/m^2 was obtained from solar measurements, which were taken on top of the surface of the specimen slab.

Radiation in solar flux can be divided into three major ranges named as visible, ultra violet and infrared. These radiations consist of different ranges of energy levels. Infrared (IR) is the most important part in solar radiation with respect to heat energy. Heat energy in solar radiation is the significant part for the thermal behavior analysis of concrete.

IR filter (Infra-Red IR Filter 720 nm – R72) which cuts down the radiation having wave lengths less than 720 nm was used to obtain the amount of solar heat flux coming with total radiation. Daystar Solar meter [16] and the IR filter were used in the separation of IR from other radiations. Fig. 2 shows the total solar radiation variation and portion of IR variation at the ground level measured from 0530 h to 1900 h in a day. The results indicate that IR is forming about 45% of the total solar radiation.

Ambient Temperature Variation

Ambient temperature is one of the parameter needed to calculate the convection heat transfer from concrete surfaces. All months with

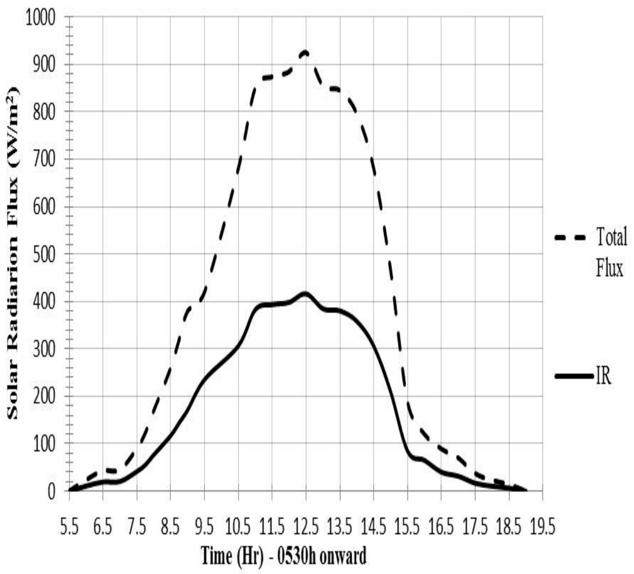

Fig. 2. Variation of Solar Radiation Components with Time.

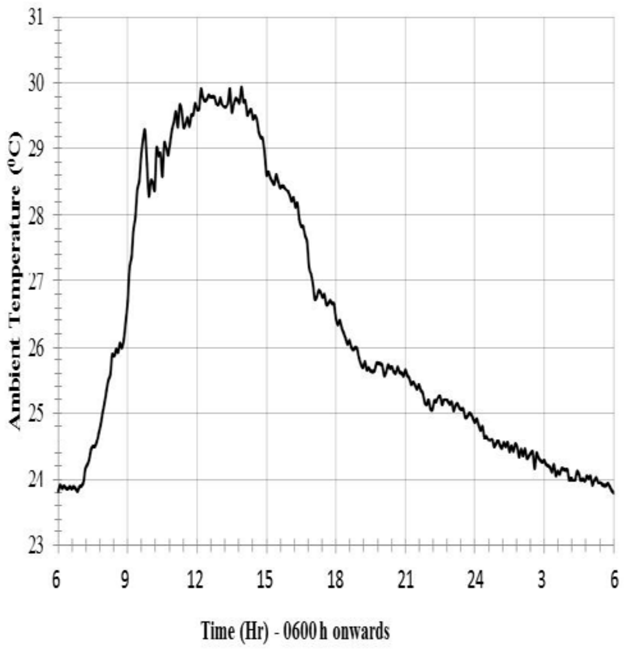

Fig. 3. Diurnal Ambient Temperature Variation.

Table 2. Properties Used for the FEM.

Property		Concrete	Soil
Thermal	Thermal Conductivity (W/m/K)	2.5	0.3
	Specific Heat (J/kg K)	700	850
Structural	Young's Modulus (N/m^2)	2.3E +10	1.2E +08
	Poison's Ratio	0.2	0.35
	Density (kg/m^3)	2400	1600

monthly mean temperatures, corrected to sea level, above 18°C is considered as the tropics [17]. In tropical countries, seasonal variations of ambient temperatures are negligible and the measurements in this study showed a variation within the range of 24 – 30°C during a typical day. Fig. 3 shows the daily ambient temperature variation at ground level measured for a 24 hour period which was incorporated in the FEM analysis.

Finite Element Model (FEM) Approach

FEM simulation of the experimental setup was used to incorporate the input values and boundary conditions for FEM to obtain the deformations at any location of the slab due to temperature variation. A coupled (thermal + structural) 3D Finite element simulation was carried out with ANSYS (Version 12.0.1), a non-linear stresses analysis software. Structural and thermal properties of concrete specimen and the boundary conditions due to environmental effects were used as input parameters.

A 150 mm thick concrete layer placed on a soil sub-grade was modelled by using ANSYS. Eight node brick element (Solid 5) was used to simulate both thermal and structural properties of concrete slab and soil-grade. Input heat flux from solar radiation on top surface and convection heat transfer from all the exposed surfaces are considered to obtain the thermal variations in concrete layer. Outcome of the coupled field analysis is structural deformation of the concrete layer due to thermal variations. Since the input parameters of the boundary conditions are varying throughout the 24 hour period, fully transient analysis was carried out for the entire period.

Input Parameters

Solar radiation variation was applied as a function which represents the portion of heat flux spread on top of the concrete pavement surface.

Free convection is a function of surrounding temperature (bulk temperature) and convective heat transfer coefficient [18]. Convective heat transfer coefficient depends on the roughness of the concrete surface, wind speed, and humidity [18]. The convective heat transfer coefficient (designated as ‘the convection film coefficient’ in ANSYS) associated with air convection is one of the most important thermal properties that is been used to represent the heat transfer between concrete surface and ambient air. Some researchers [19, 20] reported that the convective heat transfer coefficient typically ranged from 5 $W/m^2/K$ to 35 $W/m^2/K$. In this study, several test runs were carried out with different values in above range and 10 $W/m^2/K$ was selected as the convection film coefficient, which gave the most acceptable results.

The values used for thermal conductivity of concrete, specific heat of the concrete and convection film coefficient of air were verified using a separate set of temperature data and solar radiation input. Structural and thermal properties that used for the FEM analysis are given in Table 2.

Sensitivity Analysis of the Parameters Used for FEM

Sensitivity analysis of the main parameters was carried out to make the finer adjustments in the model. It was carried out by changing the main parameters; thermal conductivity and specific heat of the concrete, convection film coefficient of air, by ±20%. Table 3 shows

Table 3. Sensitivity Analysis Results of the FEM.

Parameter	Initial Value	Result (°C)	Percentage Change of Parameter	Value of Parameter after Change	Result after Change (°C)
Thermal Conductivity (W/m/K)	2.3	46.38	-20	2	46.83
			+20	3	45.28
Convection Film Coefficient ($W/m^2/K$)	10	46.38	-20	8	47.67
			+20	12	44.53
Specific Heat (J/kg K)	700	46.38	-20	560	47.08
			+20	840	44.99

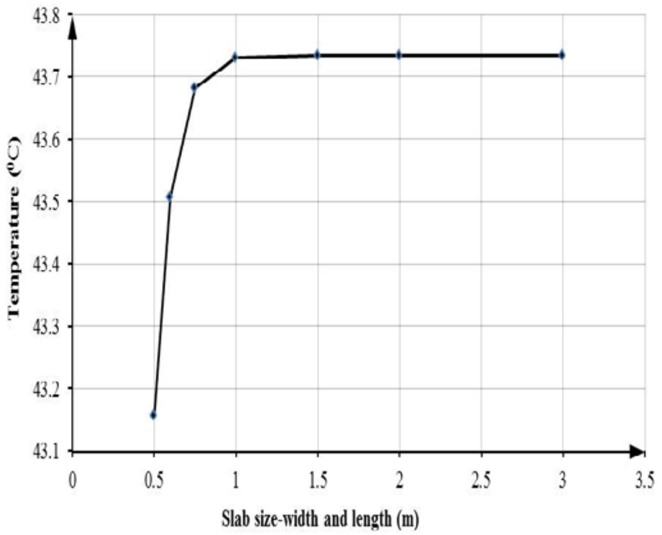

Fig. 4. Temperature Variation of the Top Surface at 1200 h with the Slab Size.

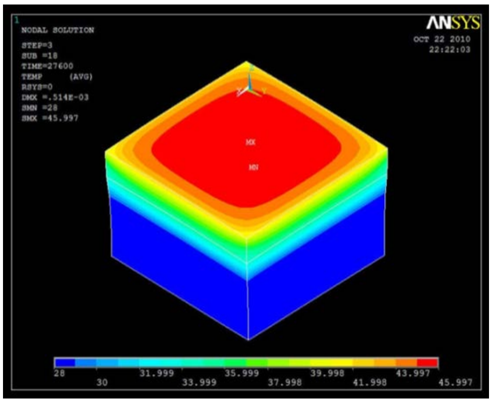

Fig. 5. Maximum Temperature in FEM.

the percentage difference of the maximum temperature results of the top surface with respect to the percentage change of each parameter. The results show that convection film coefficient is the most sensitive parameter which affects the top surface temperature, because larger surface area exposed to air and convection governs the heat dissipation. Effect of the mesh size on the finite element model was also studied Results show that the mesh size less than 10 cm is not significantly affect the FEM results. When the specific heat of concrete increased by 20%, the top surface temperature decreases by 3%. In case of thermal conductivity of concrete, 20% change of the parameter will change the top surface temperature approximately 2%.

Selection of Suitable Slab Size

A FEM developed by ANSYS software was used to select a suitable slab size for field verification of the results. In this model study, the effect of the size of the slab on the temperature at mid-point of its top surface was examined. Size of the slab panel was changed, while maintaining all other parameters constant. Fig. 4 shows the top surface temperature variation (at 12 noon) with the model size. The graph implies that the size of the slab does not affect the maximum temperature of mid-point of top surface, when the slab size becomes larger than 1 m x 1 m. Therefore, 1 m x 1 m slab was selected to verify the results.

FEM Results and Verification

A 1 m x 1 m x 0.15 m concrete slab, which was placed on top of a 0.5 m thick soil layer, was modelled with ANSYS. Fig. 5 shows the developed FEM. The top surface of the concrete layer is exposed to solar radiation during the day time and convection boundary condition was also applied for all the concrete surfaces. Fig. 5 shows the results of the FEM at the time of maximum temperature out put on top surface.

Daily temperature variation of concrete slab at selected points across the thickness of center of the slab was observed. The thermocouple was placed from top to bottom in 25 mm intervals. The distance from top surface and notations are given as; 0(Top), 25(2), 50(3), 75(4), 100(5), 125(6), and 150(Bottom).

Fig. 6 shows FE analysis results of the variation of the temperature profile across the slab thickness for 24 hour period. The time period was considered to start at 0600h as the solar heat flux begins. Concrete begins to heat up as the intensity of the solar heat flux increases and its temperature reached its maximum around 1400 h and started to cool down thereafter. Meanwhile, the bottom layers were recorded to have higher temperatures than the top surface in the evening hours. This is due to the heat loss from top surface as convection decrement of heat flux input during the said time period. Concrete slab reached its lowest temperature value at around 0600h on the next day, but never dropped down to its corresponding ambient temperature. This is because of the fact that the top surface starts to gain solar heat flux on the following day prior to the total heat dissipation of the concrete slab.

Calibration of FEM

Prototype slab Construction

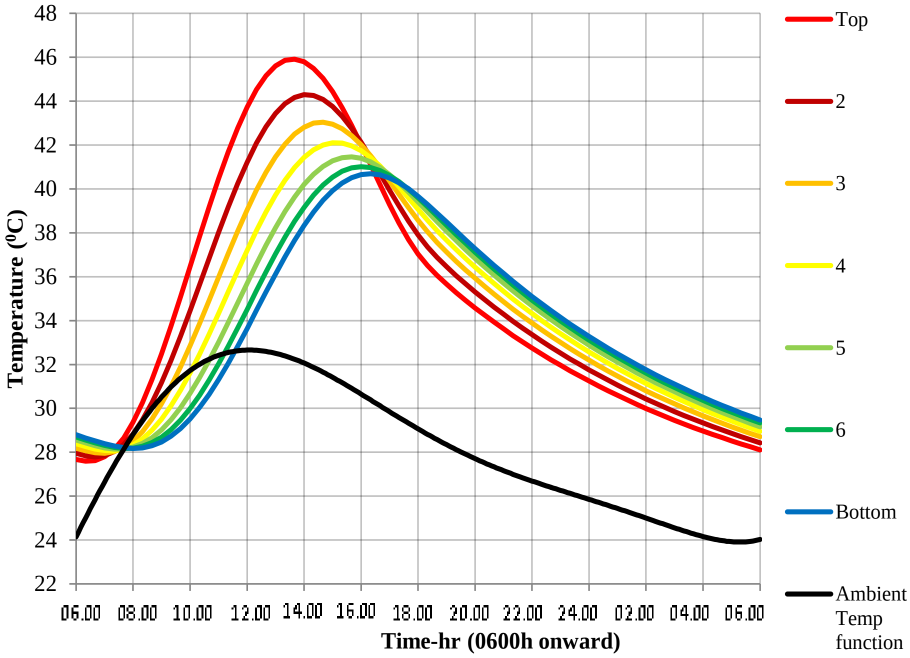

Fig. 6. FE Analysis Results of Temperature Variation Across the Thickness of 0.15 m.

(a) (b)

Fig. 7. Thermocouple Arrangement in the Slab (a) Formwork Placed on Thick Polythene Sheet, (b) Thermocouples Attached to the Formwork Using non-elastic and Thermoplastic Wire.

Fig. 8. Data Logger and Concrete Slab with Thermocouples.

Based on the FE analysis results, a prototype slab was cast for the experimental verification. The slab was placed at an open area having exposure to direct solar radiation throughout the day.

Mix design was carried out using the DOE method [21] for slump of 60 mm and average compressive strength of 25 MPa at 28 days. The used mix proportion of cement, fine aggregate, coarse aggregate were 183, 405, and 1183 kg/ m^3 respectively. Water / cement ratio and fine/ coarse aggregate ratio were maintained at 0.45 and 0.54 respectively.

A thick polythene sheet was placed between the soil and concrete to separate the layers and to prevent any loss of water from fresh concrete to soil (Fig. 7a). Thermocouples were fixed to the formwork at 25mm intervals. The spaces of inserted thermocouples were fixed using a non-elastic, thermoplastic wire (Fig. 7b). A data logger with K type thermocouples were used to measure the temperature in concrete. The data logger was set to measure the temperature at every 5 minute intervals for the entire period of testing. Ambient temperature was also measured using a separate thermocouple. Exposed concrete slab with the data logger is shown in Fig. 8.

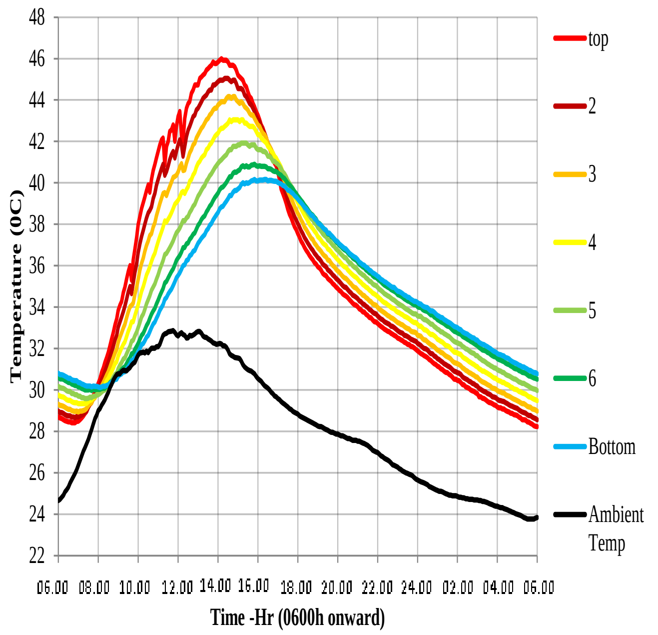

Fig. 9. Measured Daily Temperature Variation Across the Concrete Slab Thickness.

Results of the Prototype Slab

Temperature variation across the slab was obtained to compare with the FEM results. Fig. 9 shows the temperature variation of thermocouples placed in the center of the slab from top to bottom.

Comparison of the Results and Calibration of FEM

Results obtained from the FEM and the prototype slabs were

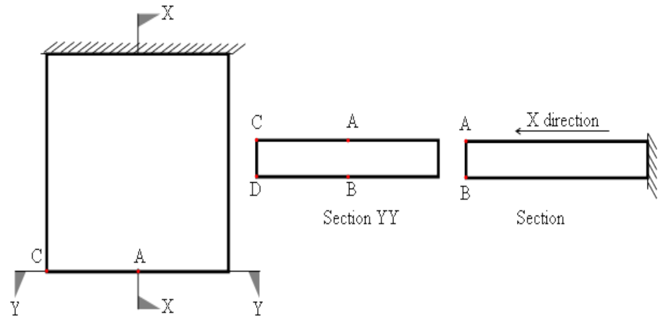

Fig. 10. Considered Points for the Deflection Readings.

compared to verify the FEM. In order to examine the consistency of the predicted temperature values by ANSYS model, Chi Squared Goodness of Fit test was conducted and it was found that the predicted temperature values fall within 95% confident level with the actual measured temperatures. Hence, it can be concluded that the predicted temperature values are consistent with the actual temperature values. Verified FEM was used to obtain the deformation of the concrete pavement slab due to daily temperature variation.

Maximum Deformation Due to Thermal Variation

Structural deformations were obtained from the verified FEM for temperature records of March to April period. One side of the concrete slab was kept fixed and the corresponding deflections were observed at the other side. Deflections of 1 m x 1 m slab were obtained at the middle top and bottom layers of the side surface and the corners. Figs. 10 and 11 show the selected points and the variation of deflection with time of the day.

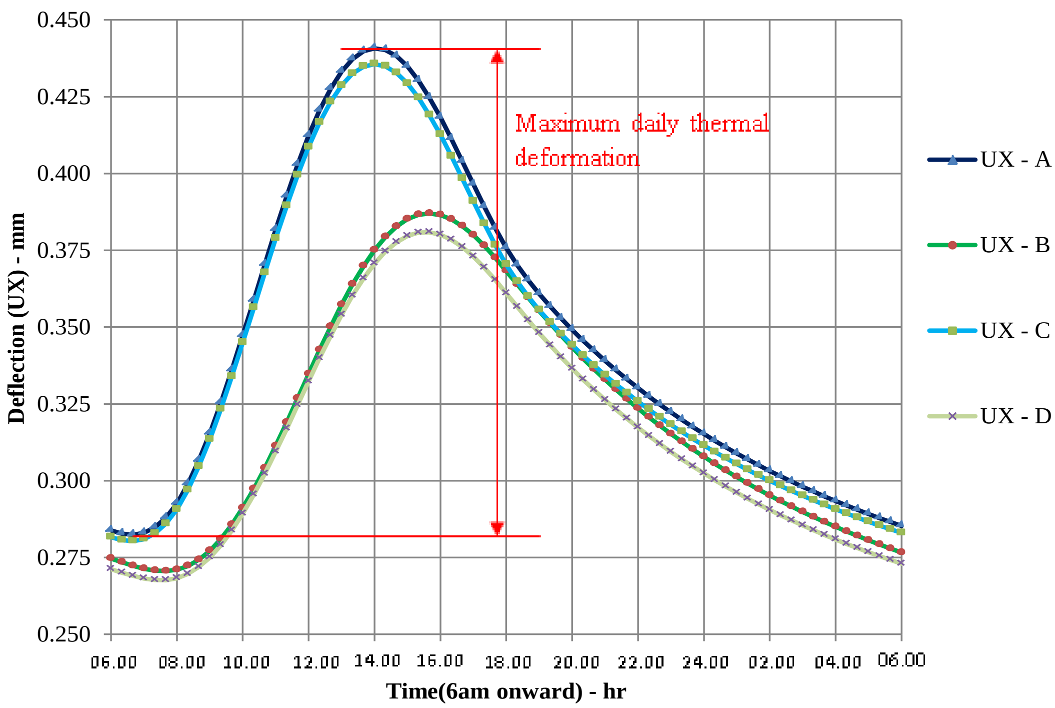

Fig. 11. Deformation of Edge of Slab with the Time of the Day.

Fig. 11 shows that concrete deformation is relatively higher during the day time than during the night time. This is due to the higher heat energy absorption during the day time, resulted due to the higher intensity of solar heat flux. The length changes with respect to original length according to the time of hardening of the concrete. If the concrete hardens at the day time, it tends to contract at the night time. If the concrete hardens at night time, it tends to expand during day time.

The worst situation occurs when the concrete hardens during the day time, as it induces tensile stresses and open up already formed crack/joints during the day time. As it can be seen in Fig. 11, the maximum possible contraction occurs at the top surface of the slab and found to be 0.16 mm/m for the temperature variation considered. This value will be incorporated in calculating an appropriate joint spacing for 150 mm thick concrete pavement slabs.

Deformation Due to Shrinkage of Concrete

In this study, the expected shrinkage strain of concrete was obtained based on the guidelines given in ACI [22]. Shrinkage of concrete depends on the restrain condition. In the case of concrete pavement slab, restrain provided by friction acting on the bottom face significantly influences the shrinkage induced tensile stress in the slab. Therefore the magnitude of shrinkage depends not only on the free shrinkage of concrete but also on interface frictional characteristics between concrete base layer [23]. By introducing a polythene layer under the slab, it is possible to reduce the friction and obtain a partially restrained state at the interface.

In this study, free shrinkage was considered, as it is the worst possible scenario that would occur in a rigid pavement. Shrinkage model given in ACI [22] was used to obtain the ultimate shrinkage for 30 year design life of 150 mm thick concrete slab. The model based on aggregate and cement percentages, curing time, slump and the relative humidity of the surrounding environment.

According to the climatic data have been recorded in Sri Lanka [24], average minimum relative humidity is about 60% and hence the shrinkage strain was calculated for the 60% relative humidity. According to the ACI [22] shrinkage model, 30 year shrinkage strain was obtained as 0.48 mm/ m.

Experimental Investigation of Load Transfer Efficiency (LTE)

LTE at the joint is determined based on the ratio of the maximum deflection at the joint of the loaded slab and the deflection of the unloaded slab measured right across the joint from the maximum deflection. According to Fig. 12, deflection based LTE can be calculated from Eq. (1) [25].

$$LTE(\%) = \frac{D_U}{D_L} \times 100 \tag{1}$$

where,

D_L = the maximum deflection at the joint of the loaded slab.

D_U = the corresponding deflection at the joint of the unloaded slab.

Rigid pavement rehabilitation guidelines [26, 27] specify the limits on performance of joint to restore the load transfer mechanisms. Deflection load transfer of 60 % or less, joint faulting

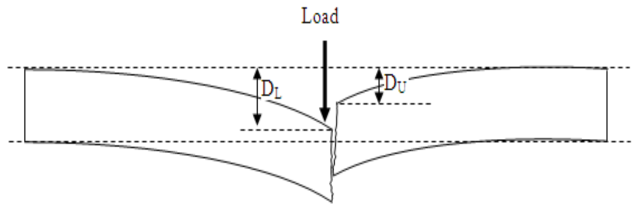

Fig. 12. Deformation of Slabs at a Joint Under Edge Loading.

less than 2.5 mm and differential deflection of 250 μm or less have been identified as the indicators for an individual joint or crack to benefit from load transfer restoration [26, 27].

In this study experimental investigation was carried out to obtain the relationship between deflection LTE and crack opening to decide the limit of crack width for the specified LTE. Deflection LTE should be kept more than 60% within the design life of the pavement. Therefore, the crack opening due to thermal variations and shrinkage effect should be kept within safe limit corresponding to 60% LTE.

Selection of Suitable Slab Size

A single wheel load of standard 80 kN single axle load was used for the experiment. Deflection based LTE changes with the load type. According to the Brink's study [28], static loading gives the lowest values for the LTE for any crack width less than 2.5 mm. In the actual condition, a vehicle tire load usually resulted in forming a dynamic load on pavement structures. As the static loading is critical in LTE, such an efficiency arising from static loading will satisfy the requirement of actual loading condition of a road pavement. Therefore, static load application was carried out to obtain the relationship between crack width and LTE.

The size of the prototype slab was decided based on FEM analysis. Slab size is a major factor governs the effect of the load application on the deflection. In this study, behaviour of stress contours was analysed to obtain the minimum size of the slab that does not affect the deflections under the applied load conditions. The pavement analysis software FEACON [12] was used to analyse a slab on ground and obtained the stress contours.

Properties of the underneath soil layer also makes significant influence on the resulting stresses and corresponding deflections. In this study, the deflection of certain pre-determined points for various slab dimensions were considered. All the other corresponding parameters for the deflection were kept constant and only the deflections of the top surface were observed. Concrete and soil properties used for the FEACON model: Elastic modulus, density and poisson ratio of concrete were 23000 MPa, 2400 kg/m3 and 0.2 respectively and subgrade modulus and density of soil (subgrade) were 85 MPa/m and 1800 kg/m^3. Fig. 13 shows the mesh, load point and selected points to check deflection of the selected slab.

Figs. 14 and 15 show the variation of deflections at points A, B, C and D with the slab size (L). The selection criterion of the suitable slab size was based on stresses at the selected points of top face. The results indicate that the size of the slab does not affect the deflection beyond the 1.5 m x 1.5 m slab size.

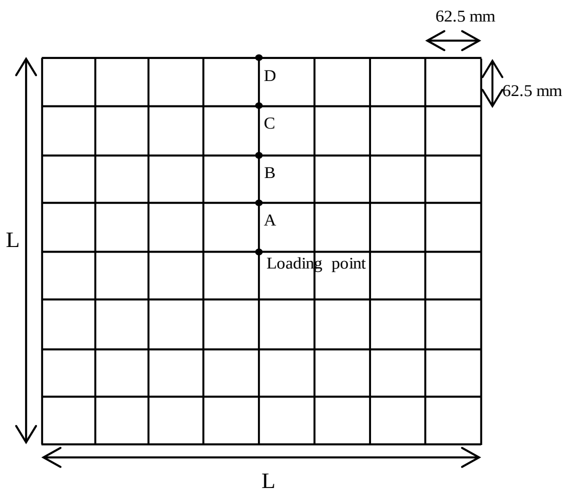

Fig. 13. Mesh and Loading Points of the Model Slab.

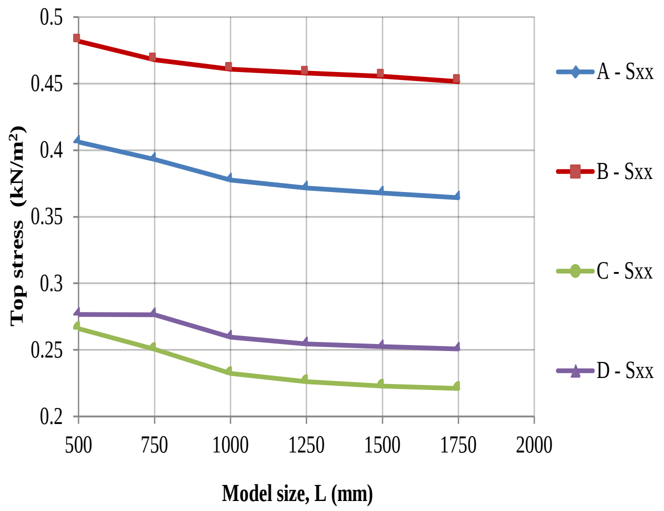

Fig. 14. Variation of Direct Stress in y Direction with Model Size (L).

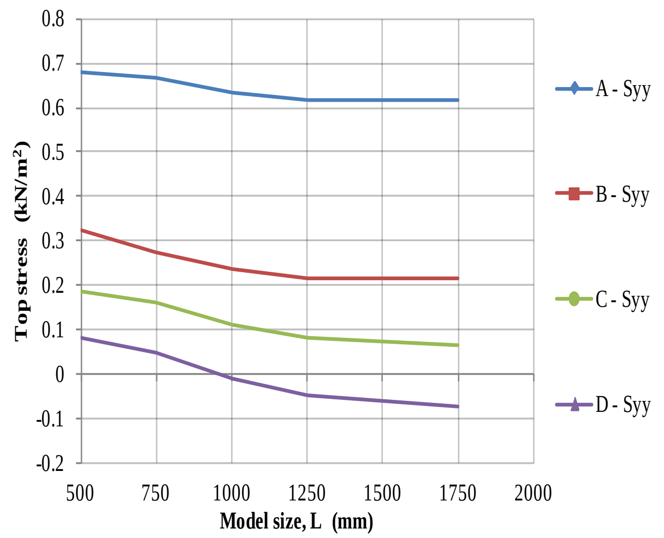

Fig. 15. Variation of Direct Stress in x Direction with Model Size (L).

Investigation on LTE Related to Crack Width

Based on the analysis, minimum required size of the slab panel was found to be 1.5 m x 1.5 m and the selected panel size was 1.75 m x 1.5 m. Grade 25 concrete with 20 mm aggregate was used to cast the test slab. Since the slab is required to test for LTE based on deflection, it is necessary to measure the deflection of the slab under applied load. In order to generate measurable deflections, slab should be supported on a flexible material. Therefore, the concrete slab was cast on a rubber pad of approximately 16 mm thickness to simulate a Winkler foundation and to provide a uniform sub-grade with continuous support.

Although the selected panel size was adequate to eliminate the dimensional effects on LTE, it cannot represent the conditions of a long slab panel under a point load. Actual pavement slab will deflect as a curve under the point load at the joint due to the restrain provided as a result of long length and subgrade friction. If the ends of a 1.5 m long slab panel are free then the ends will raise under wheel load at joint. Therefore, the two ends of the slab were fixed to the strong floor. Fig. 16 shows the sketch of the test slab.

Concrete slab with selected size was cast on top of a rubber strip. The slab was fixed into the strong floor using strong bolts. Acrylic sheet of 50 mm x 4 mm thick was placed across the middle of the slab during the casting stage. The purpose of this acrylic sheet was to make a 50 mm deep groove on the top surface where the crack should propagate. It makes a weaker plane at the middle across section. Two threaded bars are attached either side of the slab across the grove. The threaded bars are fixed into slab using 'L' section. The purpose of the threaded bars is to change the crack width as per requirement of the test. A crack was introduced by loading the slab at the center, after placing it on two steel bars.

Wheel effect of a standard axle load of 80 kN was simulated by 40 kN vertical load on 100 cm^2 area adjacent to the crack. Vertical load was applied by a hydraulic jack through a load cell, which were connected to a data logger to measure the applied load. Deflections at the selected locations were measured using transducers and mechanical dial gauges (Fig. 17).

Digital dial gauge was fixed horizontally across the crack to measure any changes of crack width. Crack width was changed from 0.25 mm to 7.00 mm in 0.25 mm intervals. Deflections on either side of the slab were recorded at each crack width. Fig. 18 shows the variation of the LTE in related to crack width.

Based on the LTE results shown in Fig. 18, the crack width at 60% LTE is 2.3 mm. Since this test was carried out under static loading, higher load transfer can be achieved for this crack width under dynamic loading conditions, which is the actual loading condition of a typical road pavement. This crack width was used in calculating an appropriate joint spacing for 150 mm thick concrete pavement slabs.

Optimum Joint Spacing for Low Volume Roads

The joint spacing can be calculated by considering daily temperature variation and drying shrinkage using Eq. (2) [29].

$$w = L\,C\,(\alpha T + \varepsilon) \qquad (2)$$

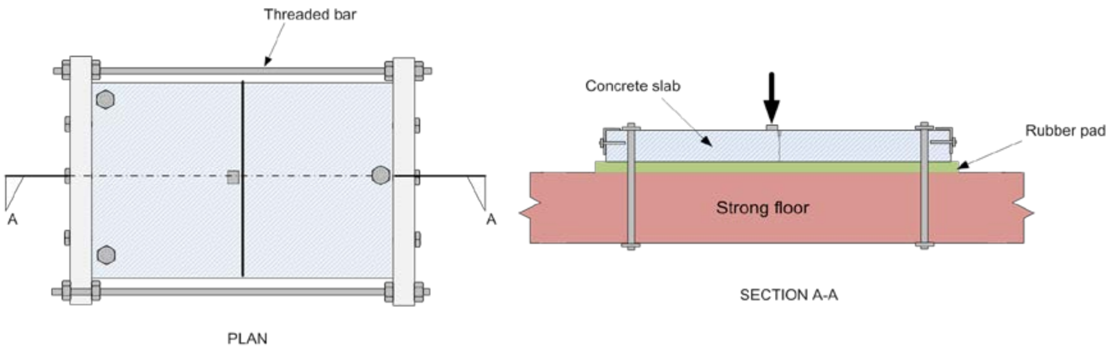

Fig. 16. Experimental Setup for the LTE Test.

Fig. 17. Deflection Measuring Arrangement.

where
w = crack width
αT = deformation due to daily temperature variation
ε = deformation due to shrinkage
L = joint spacing
C = the adjustment factor due to sub base/slab friction restraint; 0.65 for stabilized sub base, 0.80 for granular base and 1.0 for natural clay sub-grade

According to the results of the study, crack width should be less than or equal to 2.3 mm to satisfy 60 % LTE.

Table 4 shows the joint spacing calculated based on the results of this investigation for 150 mm thick concrete slab pavement under low volume traffic condition. According to the Table 4, for 3.6 m

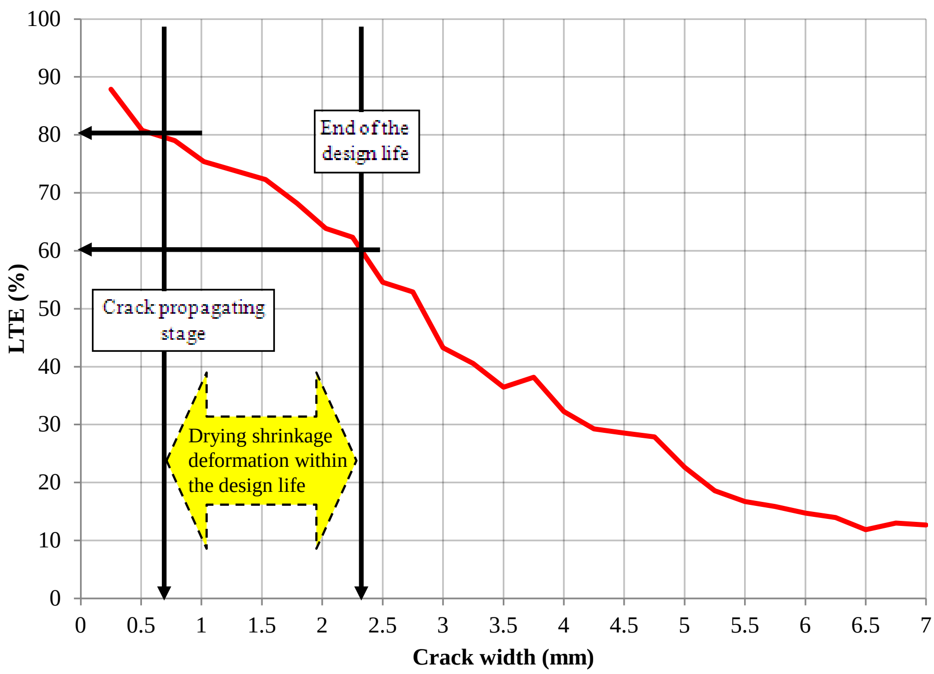

Fig. 18. LTE Variation with Crack width at Different Stages of Concrete.

Table 4. Joint Spacing for 150 mm Thick Concrete Pavement Slab.

Crack Width for 60% LTE	Daily Thermal Contraction	Shrinkage Strain	Base Type	Joint Spacing m (ft)
			Natural Clay	3.6 (12)
2.30 mm	0.16 mm/m	0.48 mm/m	Granular	4.5 (15)
			Stabilized	5.5 (18)

long slab under natural clay base will have a 2.3 mm crack opening at the end of its design life and the deflection based LTE will be 60% at that stage. Initial LTE at the time of crack propagation under saw cut (i.e. at the joint) is mainly based on the daily thermal contraction. Although, the slab has an ultimate shrinkage of 0.48 mm per meter length after 30 years' time, strain due to shrinkage at the initial stage is negligible (Neville, 1996). Therefore, the effect of shrinkage at the early age of concrete on crack width may not be significant and the only effect to be considered at early age is the maximum daily thermal contraction due to daily variation of solar radiation. Thus, the crack opening due to daily thermal contraction will be 0.5 - 0.88 mm for the given base types in Table 4. Load transfer efficiency at the crack propagating stage was obtained about 80% from Fig. 18. As the drying shrinkage of concrete increases, crack opening will also be widened. At the end of its design life (i.e. 30 years), the maximum crack opening due to both shrinkage and thermal movements was considered to be 2.3 mm for the joint spacing design which corresponds to the 60% LTE. Therefore, it can be stated that the LTE reduces from 80% to 60% during the expected life span of the slab.

Conclusion

The procedure described in this study can be used to design the joint spacing in non-dowelled rigid pavements. It requires the daily ambient temperature variation, solar heat input at the location, relative humidity data and sub base/slab friction restraint to calculate the expected longitudinal contraction of the non-dowelled rigid pavement.

Daily temperature variation and shrinkage are the most influencing factors affecting crack width and hence the joint spacing in non-dowelled rigid pavements. Daily temperature variation causes the pavement expansion, contraction and curling. Pavement contraction leads to the crack widening and also decreases the LTE.

In this study, daily temperature variation of a concrete slab was incorporated in a FEM to obtain deformation and was also verified using a prototype slab. The maximum daily contraction was obtained as 0.16 mm/m from the verified FEM. Shrinkage strain of concrete was obtained from the shrinkage model given in ACI [22]. Ultimate value of the shrinkage strain was obtained as 0.48 mm/m for 150 mm thick slabs.

In pavement management, LTE has to be maintained above 60% to ensure acceptable pavement serviceability. An experimental investigation was carried out to obtain the relationship between LTE and crack width. Based on the relationship developed, the maximum possible crack width to keep LTE above 60% is 2.3 mm.

Based on daily thermal variation and expected free drying shrinkage of concrete, the recommended joint spacing for low volume roads of 150 mm thickness in tropical climate is 3.6 m, 4.5 m and 5.5 m for natural clay sub-grade, granular sub base and stabilized sub-base respectively. These results confirm the ACPA [7] recommendation for joint spacing for rigid pavement with 150 mm thickness which is 3.7 - 4.6 m.

The result of this study gives higher value than the rule of thumb value given in rigid pavement design guidelines for the United States. Federal Aviation Administration in U.S. Department of Transportation has recommended that joint spacing in feet is twice the pavement thickness in inches, which produces a joint spacing of 3.7 m (12 feet) for 150 mm (6 inches) thick pavement. This implies that the thumb rule is reasonably equivalent with the results of this study for the natural clay sub-bases. The non-dowelled rigid pavement construction can be done at a higher joint spacing in tropical climate than the above specifications by using a rough sub-grade of granular or stabilized soil to maintain a higher level of LTE in concrete slab. It would be a cost effective approach as higher the joint spacing means lesser the construction effort and cost.

References

1. NCHRP (2004). Guide for Mechanistic- Empirical Design of New and Rehabilitated Pavement Structures, in *NCHRP 1-37A Final Report*, National Cooperative Highway Research Program, National Research Council, Washington, DC, USA.
2. Neville, A.M. (1996). *Properties of concrete*. 4th edition, John Wiley & Sons, Inc., New York, USA.
3. ACPA (1994), Concrete Pavements with Un-doweled Joints for Light Traffic Facilities, in *IS405.01P1994*, American Concrete Pavement Association, Washington, DC, USA.
4. Colley, B.E. and Humphrey, H.A. (1967). Aggregate Interlock at Joints in Concrete Pavements. *Highway Research Record*, No. 189, pp. 1-18.
5. Strahler, A.N. and Strahler, A.H. (1989). *Elements of physical geography*, 3rd Ed., John Wiley & Sons, New York, USA.
6. AASHTO (1993). AASHTO Guide for Design of Pavement Structures, American Association of State Highway and Transportation Officials (AASHTO), Washington, DC, USA.
7. ACPA, Design of Concrete Pavement for City Streets, in IS184P1992: American Concrete Pavement Association.
8. IDOT, Standard Road Plans, in Iowa Department of Transportation1989: Highway Division, Office of Road Design.
9. Larson, R.M, Peterson, D., and Correa, A. (1998). Retrofit Load Transfer Special Demonstration Project SP-204, *Report No. FHWASA- 98-047*, Federal Highway Administration, Washington, DC, USA.
10. MnDOT (1982). Road Design Manual, Minnesota Department of Transportation: Office of Project Management and Technical Support, Saint Paul, Minnesota, USA.
11. Tia, M., Ruth, B.E., Wu, C.L., and Eom, K.S. (1986). Field Evaluation of Rigid Pavements for the Development of a Rigid Pavement Design System –Phase I. Department of Civil Engineering: College of Engineering, University of Florida, Gainesville, FL, USA.
12. Tia, M., Ruth, B.E., Wu, C.L., and Eom, K.S. (1987). Field Evaluation of Rigid Pavements for the Development of A Rigid Pavement Design System –Phase II. Department of Civil Engineering: College of Engineering, University of Florida, Gainseville, FL, USA.
13. Tia, M., Bloomquist, D., Ruth, B.E., Wu, C.L., Choubane, B., and Tang, C.H. (1988). Field Evaluation of Rigid Pavements for the Development of a Rigid Pavement Design System –Phase III. Department of Civil Engineering: College of Engineering, University of Florida, Gainesville, FL, USA.

14. Karunarathne, A.M.A.N. (2011). Design of Rigid Pavement Joint Spacing for Low Volume Roads, *MS Thesis*, University of Moratuwa, Sri Lanka.
15. AL-Dallal, S. and Zein, M. (1986). Measurement of Solar Spectrum in Bahrain. In: ALAWI, H. (ed.) Solar Energy Prospect in the Arab World: Second Arab International Solar Energy Conference. Bahrain, pp 86-90.
16. DAYSTAR (2009). The Daystar Solar Meter - DS-05A [Online]. http://www.zianet.com/daystar/solarmeter.html. [Accessed 05-09- 2009].
17. Velthuizen, H.V., Huddleston, B., Fischer, G., Salvatore, M., Ataman, E., Nachtergaele, O.F., Zanetti, M., and Bloise, M. (2007). Mapping biophysical factors that influence agricultural production and rural vulnerability. Environment and Natural Resources Series. Rome: Food and Agriculture Organization of the United Nations and International Institute for Applied Systems Analysis.
18. Lee, Y., Choi, M.-S., Yi, S.-T., and Kim, J.-K. (2009). Experimental study on the convective heat transfer coefficient of early-age concrete. *Cement and concrete composites*, 31, pp. 60-71.
19. Hsieh, C., Qin, C., and Ryder, E. (1989). Development of computer modeling for prediction of temperature distribution inside concrete pavements. FL/DOT/SO/90-374. Mechanical Engineering Department, University of Florida, Gainesville, FL, USA.
20. Rubinsky, I.A. (1954). Heat of hydration in concrete. *Magazine of Concrete Research*, 6, pp. 79 –92.
21. Teychennee, D.C., Franklin, R.E., and Erntroy, H.C. (1988). *Design of Normal Concrete Mixes*, Building Research Establishment, Watford, UK.
22. ACI 209R-92 (1997). Prediction of creep, shrinkage and temperature effects in concrete structures, *ACI Manual of Concrete Practice, Part 1: Materials and General Properties of Concrete*, Detroit, Michigan, USA.
23. Zhang, J. and Li, V.C. (2001). Influence of supporting base characteristics on shrinkage-induced stresses in concrete pavements. *Journal of Transportation Engineering*, 127, pp. 455-462.
24. Khazanovich, L. and Gotlif, A. (2003). Evaluation of Joint and Crack Load Transfer Final Report, *Report No: FHWA-RD-02-088*, Federal Highway Administration, Washington, DC, USA.
25. Jayasinghe, C. and Jayasinghe, T. (2009). *Sustainable Design of Built Environments*, Eco Ceylon (Pvt.) Limited, Colombo, Sri Lanka.
26. Federal Highway Administration. (1997). Concrete Pavement Rehabilitation - Guide for Load Transfer Restoration, *Report No: FHWA-SA-97-103*, Federal Highway Administration, Washington, DC, USA.
27. Bautista, F.E. and Basheer, I. (2008). *Jointed Plain Concrete Pavement (JPCP) Preservation and Rehabilitation Design Guide*, Pavement Design & Analysis Branch, Office of Pavement Design: Division of Design, California Department of Transportation, California, USA.
28. Brink, A.C., Horak, E., and Visser, A. (2005). Improvement of Aggregate Interlock Equation Used in Mechanistic Design Software, International Journal of Concrete Pavements, 1(1), pp 1-22.
29. Darter, M.I. and Barenberg, E.J. (1977). Design of zero maintenance plain concrete pavement, Vol. II-Design Manual - *FHWA-RD-77-112*. Federal Highway Administration, Washington, DC, USA.